Determining the Contribution of Shaded Elements of a Canopy to Remotely Sensed Hyperspectral Signatures

H. Peter White[1], Lixin Sun[2], Karl Staenz[1], Richard Fernandes[1], Catherine M. Champagne[3]
1) Canada Centre for Remote Sensing – Natural Resources Canada, Ottawa, ON, Canada, K1A 0Y7
2) Dendron Resources Surveys Inc., Ottawa, ON, Canada, K1Z 5L9
3) MIR Télédétection Inc., Québec, PQ, Canada, J4K 1A3
Contact Email: PWhite@NRCan.GC.Ca

ABSTRACT - *Hyperspectral imagery has the potential to become a useful tool for monitoring and extracting biophysical properties of vegetated areas. Exploitation of this potential relies on the ability to relate at-canopy spectral reflectance to biophysical characteristics of vegetation and derive both sunlit and shaded component proportions and spectral profiles. Increased application of hyperspectral imagery to these areas is expected with the advent of space borne hyperspectral sensors (such as EO-1 Hyperion and CHRIS-PROBA). Such imagery of vegetated scenes is influenced however by the well known bidirectional reflectance distribution (BRDF) effect.*

<p>One method of determining the contribution of shaded overstorey vegetation and background to observed spectral reflectance is to determine, by model inversion, the proportion of shaded surfaces viewed by the sensor, and the relative intensity of the radiative flux incident on these surfaces. This can be achieved by modelling the overall reflectance as composed of mean sunlit and shaded reflectance components, combined with an analytical description of the shaded radiant flux. Assuming a land cover type with consistent mean foliage and background reflectance, inversion of a semi-empirical model can be used to determine BRDF coefficients, which can then be applied to normalize the imagery to a specific view/sun geometry. If the modelled spectral coefficients directly relate to canopy properties, then BRDF normalization can also provide information to help directly relate the canopy architectural and biophysical properties to the remotely sensed signal. One such model, FLAIR, has been successfully used to investigate canopy characteristics from airborne and satellite spectral imagery.

1 INTRODUCTION

With the addition of hyperspectral sensors to the variety of spaceborne remote sensing instruments presently orbiting the Earth, an extra dimension of detail has become more accessible to remote sensing scientists. While hyperspectral sensors have existed for many years, they have remained part of airborne and near-surface investigative efforts until recently, with the launch of EO-1 Hyperion and CHRIS-PROBA missions. Future planned launches of ARIES and NEMO demonstrates the interest of the scientific and environmental communities in utilizing hyperspectral imagery of land surfaces on a more continual bases.

One common application of spaceborne remote sensing imagery is to relate the remotely sensed broadband signals to biophysical properties of vegetative surfaces (for example see [Badhwar et al., 1996; Abuelgasim et al., 1998; Bicheron and Leroy, 1999; and Chen et al., 2002]). While this has been a successful approach for many applications, these studies have been faced with the challenge of accounting for the anisotropic characteristics of vegetative surface reflectance, the bidirectional reflectance distribution function or *BRDF*, where the observed reflectance is influenced by both the view angle of the sensor and the location of the sun (solar angle) [for example, see Goel, 1988, White et al., 2001].

Unlike broadband studies which relate biophysical properties to reflectance magnitude, hyperspectral data has the potential to relate high resolution spectral features to their associated canopy properties. Previous studies have already noted how increased spectral information can improve the ability to relate multi-angular data to canopy properties [Abuelgasim et al. 1996; Peddle et al, 1999; Broge and Leblanc, 2000; White et al, 2001] Indeed, investigations relating spectral features directly to canopy biophysical and architectural properties have

already demonstrated significant potential [Zarco et al., 1999; Champagne et al., 2001]. But like broadband reflectance, these spectral features are also influenced by the canopy *BRDF* phenomena.

The FLAIR Model (Four-Scale Linear Model for AnIsotropic Reflectance) was initially designed to model these angular influences on canopy reflectance (the bidirectional reflectance factor, or *BRF*) [White et al., 2001; 2002]. Based on a physical description of canopy structure (as detailed by the Four-Scale Model of Chen and Leblanc [1997]), the FLAIR model is also designed for inversion of multi-angular *BRF* to provide quantitative information about the observed canopy. Thus the influences of shade and multiple scattering on the observed reflectance is used in part to relate biophysical characteristics to canopy *BRF*. Indeed, the importance of determining the shaded spectral properties has been noted in several studies [for example, see Hall et al, 1995; Peddle et al., 1999; Beaudet et al., 2002; Sabol Jr. et al., 2002]

The influences of foliage and background multiple scattering changes as a function of wavelength. For example, scattering is minimal in the red spectral region, but significant in much of the near infrared. Thus shaded contributions to the observed *BRF* are spectrally dependant, providing important information towards the determination of foliage density (i.e., effective *LAI*). By including wavelength dependant scattering properties to FLAIR inversion, an additional constraint is applied. Plus, by using the dynamic range of scattering regimes available with hyperspectral bidirectional reflectance (BRF_λ), biophysical characteristics of a canopy have the potential of being determined without the need for significant multi-angular acquisitions.

Multi-scattering influences on the BRF_λ are here modelled by determining the downwelling irradiance on shaded components of a canopy using the two-stream radiative transfer described by Sellers [1985; 1987]. FLAIR inversion of several spectral bands simultaneously now has additional constraints on the magnitude of the contribution of shaded surfaces to the observed BRF_λ. This FLAIR inversion procedure is presently being implemented with the Imaging Spectrometer Data Analysis System (ISDAS) processing software [Staenz et al., 1998] developed at the Canada Centre for Remote Sensing – Natural Resources Canada, and an agricultural test site is being used as a validation site for this procedure.

2 FLAIR INVERSION

2.1 The FLAIR Model – A Brief Review

FLAIR expresses the canopy bidirectional spectral reflectance factor (BRF_λ) as the weighted sum of four scene component mean spectral reflectance factors (shaded overstorey – R_{zt_λ}, shaded background – R_{zg_λ} sunlit overstorey – R_{t_λ}, sunlit background – R_{g_λ}), expressed as:

$$BRF_\lambda = R_{zt_\lambda} k_{zt} + R_{zg_\lambda} k_{zg} + R_{t_\lambda} k_t + R_{g_\lambda} k_g \qquad (1)$$

Spectral reflectance factors are defined as the ratio of nadir reflected radiance from a scene component to the nadir reflected radiance from a 100% Lambertian panel located at the top-of-canopy directly above the target. The four kernels (k_x) define the viewed scene component proportions, functions of the effective leaf area index (*eLAI*) [Chen et al., 1991] and the view/sun geometry ($k_x \equiv k_x(eLAI;\ \theta_v,\varphi_v,\theta_i,\varphi_i)$). For more information on the FLAIR model see White et al. [2001; 2002].

Shaded reflectance factors are now constrained using a two-stream radiative transfer algorithm to derive the downwelling irradiance intensity at the shaded surface relative to the top-of-canopy. Multi-scattering ratios are defined for both the overstorey and background as R_{zt}/R_t and R_{zg}/R_g respectively.

2.2 Modified Simplex Method for FLAIR Inversion

When limited to one spectral band, variations in observed reflectance from multiple view/sun angle image acquisitions demonstrates the influence of architecture on canopy *BRF*. When multiple spectral bands are inverted concurrently, the spectral scattering characteristics of the canopy components also become relevant. This limits the range of potential canopy architectural influences which can result in the observed BRF_λ.

With hyperspectral imagery, consisting of over 150 spectral bands, it becomes computationally expensive and redundant to invert all bands. Instead, inversion uses spectral bands (~10) which do not correlate within the spatial region of interest (ROI). When the purpose is to examine a specific spectral feature, inversion begins using uncorrelated bands over the whole hyperspectral range of the sensor, then is repeated for bands related to the spectral feature using the previous resulting reflectance factors and *eLAI* as additional constraints.

Inversion of FLAIR is performed using a modified simplex method (for a full description of the simplex method, see Vetterling et al. [1990]), where spectral reflectance factor constraints are defined using the observed BRF_λ, kernels determined for a given *eLAI* and view/sun geometry. The process continues iteratively over values of *eLAI* until a minimum constraint volume is reached.

The modified simplex method is applied by defining a 4*b* dimensional space defined by the four reflectance factors coefficients for each spectral band,

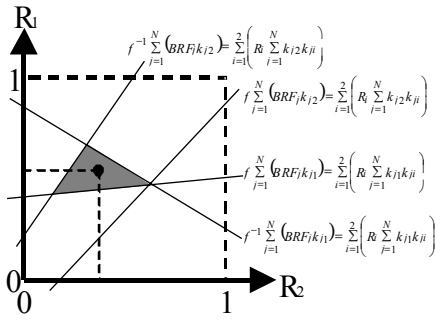

Figure 1 : Example modified simplex inversion of a two kernel, two reflectance system. Secondary constraints are indicated by their equations. As *f* decreases, so does the minimal constraint volume, represented by the grey area. The black dot indicates the reflectance values reported by the inversion procedure for this case.

b. Primary constraints are defined for each dimension based on the allowed range of each reflectance factor ($0 \le R_x \le 1$ to start, can be adjusted based on user input or model examination of data as will be outlined.).

Secondary constraints are then defined for each band based on the view/sun angular orientation (per pixel) and observed BRF_λ. For each spectral band (from *N* image acquisitions), four secondary constraints are determined. A discrepancy factor, *f*, is applied to the secondary constraints to provide upper and lower limits to the quality of the inversion, which doubles the number of secondary constraints (see figure 1). These secondary constraints define hyperplanes in the 4*b* dimensional component reflectance space. When *f* is large, the hyperplanes will not define a closed bound volume within the boundaries of the primary constraints. On the other hand, when *f* is small, then no individual volume will be bound by all hyperplanes.

An inversion iteration is complete when a value of *f* is found (if it exists) where all hyperplanes act as boundaries to the minimum constraint volume. As the procedure iterates over values of *eLAI* the minimum constraint volume will decrease (*f* approaches unity) as the value of *eLAI* approaches values reasonable for the canopy. In this way, FLAIR inversion provides discrepancy factors, *f*, as a function of *eLAI*. The resulting values of *eLAI* and component reflectance factors for the minimum value of *f* are selected as the most probable values for the canopy. If BRF_λ values are chosen from a spatial region, then the inversion results will represent average values for that region. Additional information on the inversion process can be obtained from White et al. [2001; 2002].

2.3 Simplified Modified Simplex Method Example

As an example to the inversion procedure, consider a hypothetical surface with two component constituents describable by two kernels (k_1, k_2) with two distinct reflectance factors (R_1, R_2) and no shadowing. Let there be *N* image acquisitions taken in one spectral band. In this case, the modified simplex inversion procedure would be defined in two reflectance dimensions, with four secondary constraints. For each *eLAI* iteration, the modified simplex method results in the smallest discrepancy factor, *f*, where the constraint volume remains bounded by all secondary constraints, as shown in figure 1.

As *eLAI* approaches a value reasonable for this hypothetical canopy, *f* approaches a minimum value (and the minimal constraint volume approaches zero). Inversion is complete when a global minimum of *f* is determined, and the reflectance factors which fall within that volume are reported.

3 MULTI-SCATTERING RATIO

With a focus on improving the extraction of shaded contributions to the observed spectral reflectance while simultaneously determining the radiant flux levels in this shaded canopy proportion, FLAIR inversion was further constrained with a two-stream radiative transfer model. The multi-scattering ratio is defined by the relative intensity of downwelling irradiance within a canopy on surfaces where the direct solar beam is not incident (i.e., shaded surfaces). Diffuse and direct radiative flux incident at the top-of-canopy will scatter throughout the canopy as multiple reflectance events from plant and background surfaces occur. To derive the relative magnitude of the downwelling diffuse irradiance incident on the shaded canopy components, the two-stream radiative transfer model detailed by Sellers [Sellers, 1985; 1987] is incorporated into the FLAIR inversion algorithm.

FLAIR inversion is performed, and the resulting mean sunlit spectral reflectance factors and mean *eLAI* are used to determine the mean shaded spectral reflectance factors via the two-stream model. If FLAIR derived shaded reflectance factors are outside a pre-set range when compared to the two-stream model derived values, then the primary constraints assigned to the sunlit reflectance factors are modified and inversion is repeated. If FLAIR inversion results in an extremely bright sunlit surface and dark shaded surface (relative to the two-stream model) then the sunlit reflectance factors are constrained to lower values. Alternatively, if the derived sunlit reflectance factors are low, with bright shaded areas then the

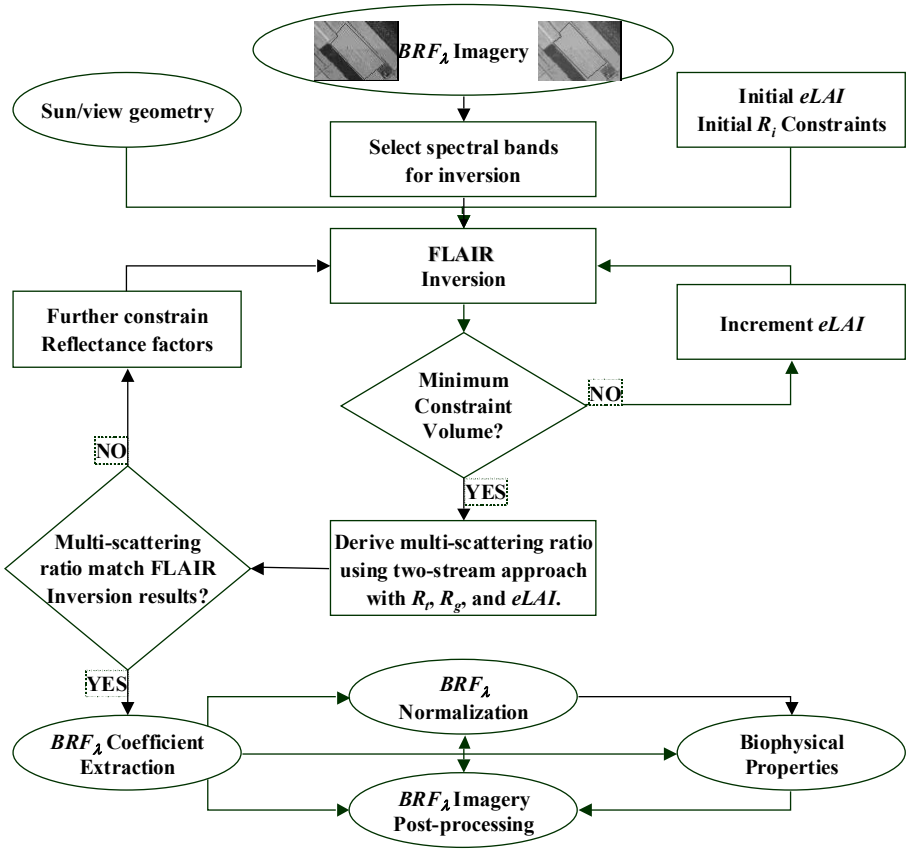

Figure 2: Processing sequence for FLAIR inversion of multi-angular hyperspectral imagery as will be implemented as a procedure in ISDAS (Imaging Spectrometer Data Analysis System developed at Natural Resources Canada – Canada Centre for Remote Sensing).

lower constraint to the sunlit reflectance factors is raised. Thus a physical constraint is given to the contribution of shaded components to observed canopy BRF_λ.

The two-stream radiative transfer model presented by Sellers [1985; 1987] follows from the work of Dickinson [1983], where the upward and downward diffuse irradiance within a canopy is modelled for a random foliage distribution with isotropically reflecting leaf elements. Both diffuse sky and direct sun at the top-of-canopy are modelled as contributing to the incident radiative flux. Leaf elements reflectance and transmittance properties are assumed equal at this stage of development with FLAIR inversion. (Further research will examine separating the foliage reflectance and transmittance within the multi-scattering model, important in the highly reflective near infrared region.)

For sunlit viewed canopy components, FLAIR inversion assumes that the direct beam intensity dominates the downwelling incident flux incident on the sunlit surface. For the shaded proportions however, the two-stream model is applied to determine the apparent shaded reflectance factor (as defined in Section 2.1). As the absolute canopy component reflectance property does not change as a function of the downwelling irradiance, the ratio of shaded-to-sunlit apparent reflectance factors can be modelled using the relative intensity of the shaded irradiance determined via the two stream model.

4 THE FLAIR INVERSION ALGORITHM

FLAIR Inversion is presently being designed as a tool for the Imaging Spectrometer Data Analysis System (ISDAS) processing software [Staenz et al., 1998]. This tool will allow the user to highlight spatial regions of interest (ROI) from hyperspectral imagery. It would then invert observed BRF_λ for selected spectral bands to determine mean *eLAI* and mean

spectral reflectance factor coefficients for the overstorey and background (including the apparent shaded spectral reflectance factors).

Inversion accuracy will depend in part on the homogeneity of the ROIs, the accuracy of the reflectance determination (atmospheric correction and sensor radiometric accuracy), as well as the range of spectral and angular variation available from the imagery. A flow chart highlighting the inversion procedure is provided in figure 2.

5 AGRICULTURAL TEST SCENE

Initially, FLAIR inversion was designed for multi-angle, single band applications. Testing of the single band inversion procedure were successfully performed using multi-angle acquisitions of forest scenes obtained during BOREAS 1994 campaigns [Sellers et al., 1995] using CASI, PARABOLA, and POLDER sensors [White et al., 2001; Leblanc et al., 2002; White et al., 2002].

Re-analysis of this boreal forest broadband *BRF* data, using the above multi-band procedure resulted in biophysical parameter and component reflectance extraction which better reproduced the concurrently measured field data [White et al., 2002].

In practice, hyperspectral image acquisitions seldom provides several distinct view angle observations of a region. Often, a sensor is flown only once, or if funds and atmospheric conditions permit, twice per study period. With satellite imagery, the acquisition is limited to the capability and orbital constraints of the sensor, limiting the sun/view geometry The present multi-band FLAIR inversion was tested on limited sun/view geometry hyperspectral imagery of agricultural scenes.

BRF_λ values were extracted from double pass airborne nadir imagery acquired over corn fields near Clinton, Ontario, using the Probe-1 sensor [Earth Search Sciences Inc., 2002] in July, 1999. The imagery consists of 128 spectral bands ranging from 430 to 2500 nm, with a pixel resolution of 5 x 5 m^2. Acquisitions were 45 minutes apart, resulting in a change of solar zenith angle from 43° to 35°. In-field measurements of corn leaf reflectance and *eLAI* were taken concurrently [Champagne et al., 2002].

To provide sufficient data for inversion, a ROI was defined outlining corn fields in the test image area known to be of similar age and subject to similar growing conditions. View/sun geometry for each pixel with the ROI was determined, and corn field BRF_λ extracted. FLAIR inversion was performed as outlined above. Sample results of the inversion procedure are provided in figure 3.

The inverse derived mean *eLAI* of the validation corn field is within the standard error of the mean *eLAI* measured in-field of 2.4±0.3 [Pacheco, 2001] using a LI-COR LAI-2000 [LI-COR, 1992]. GER3700 Spectroradiometer [GER Corp., 2002] reflectance measurements of sunlit corn leaves measured at the Clinton sites are also reproduced by FLAIR inversion.

Visual inspection of the results easily reveal however that the sunlit background spectral

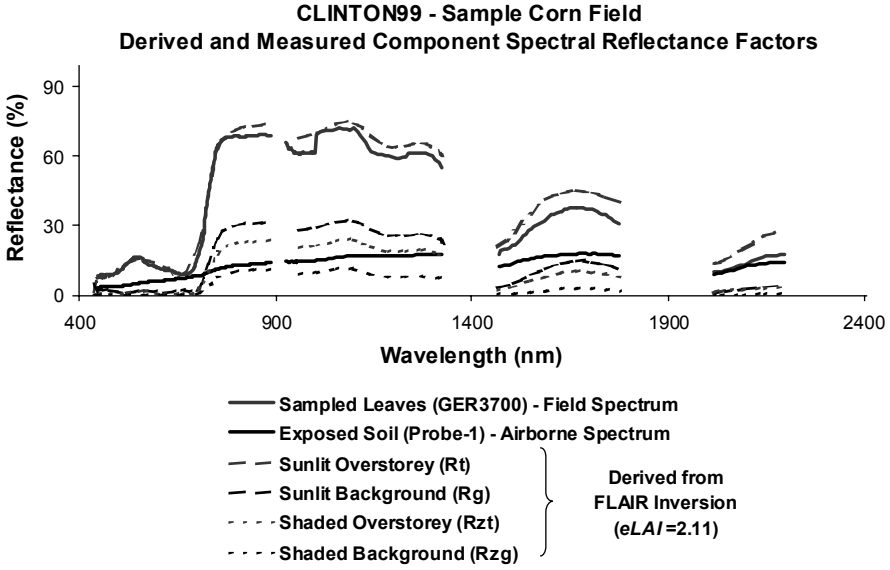

Figure 3: FLAIR inversion derived component spectral reflectance factor signatures of a Clinton test corn field. Field data spectral reflectance factors (GER3700) are provided for comparison.

reflectance factors do not match. While the magnitudes are similar, the inversion derived background reflectance maintains a vegetation-like signature not seen with the bare soil spectral nadir reflectance. This may be due in part to the existence of ground cover plants (weeds) and residue in the fields which were not present at the bare soil site used to obtain the sunlit soil spectral reflectance. Also of note, the selected sunlit bare soil site was not contaminated by contributions of foliage multi-scattering to the incident downwelling flux on not-shaded background locations, further research is required to determine the relative influence of this contribution to the observed reflectance. Shaded spectral reflectance derived by FLAIR inversion are also shown in figure 3.

One example application of utilizing hyperspectral inversion is sub-pixel unmixing, using a spectral mixing analysis. A previous analysis of this data [Pacheco et al., 2001] performed a constrained linear spectral unmixing of the Clinton corn fields to determine the percentage of crop per pixel. The aim was to identify areas of high and low yield and to compare unmixing results to measured *eLAI*.

Table 1: Endmember fractions using various analysis techniques of the Clinton test corn field from sample plot locations.

	From Vertical Photographs		Using Image Endmember Extraction		Using FLAIR Endmember Extraction	
Site ID	Soil	Corn	Soil	Corn	Soil	Corn
377-38	0.19	0.81	0.03	0.97	0.18	0.82
362-57	0.22	0.78	0.02	0.98	0.09	0.91
343-80	0.14	0.86	0.01	0.99	0.11	0.89
331-95	0.13	0.87	0.02	0.98	0.14	0.86
315-101	0.21	0.79	0.06	0.94	0.23	0.77
Scene Average	0.18	0.82	0.03	0.97	0.15	0.85

In that study, endmember spectra were selected by identifying areas of clear soil and dense foliage and extracting their spectral reflectance from the hyperspectral imagery. Table 1 shows pixel specific results of unmixing a Clinton test corn field using endmembers selected using the original field observed endmember spectra, as well as by using FLAIR inversion results as endmembers. For comparison, digital camera imagery analysis of the identified pixels are also shown. FLAIR endmembers included both shaded and sunlit spectral reflectance factors for the overstorey and background, for comparison to previous studies, the shaded and sunlit fractional components are combined in table 1.

4 DISCUSSION

This preliminary investigation demonstrates the potential of using BRF_λ inversion to determine average scene *eLAI*, component spectral reflectance factors, and shaded properties of agricultural corn crops. This analysis used the previously demonstrated (for forest canopies) FLAIR Model with the addition of a two-stream radiative transfer model to constraint the contribution of shaded components to the observed reflectance.

When the scene is sufficiently homogeneous in composition, such as an agricultural field, then the derived mean component spectral reflectance factors can be directly related to the foliage and background. This allows for the definition and separation of sunlit and shaded spectral signatures which can be used for such things as spectral unmixing and determining shaded light conditions at the understorey level.

More detailed investigation of this technique with other agricultural crops and more heterogeneous canopies will be pursued. Of specific interest will be the examination of how canopy *BRF* is influenced with respect to spectral features (such as the water index which relies on determining the accurate depth of liquid water absorption features [Peñuelas et al., 1986], the red-edge spectral features used for land cover mapping [Zarco-Tejada and Miller, 1999]) and the level of light intensity in shade within a vegetative canopy (significant for determining such properties as secondary growth success (weeds in agricultural crop) and successional processes (second generation tree growth in forests)).

5 ACKNOWLEDGEMENTS

The authors would like thank Abdelgadir Abuelgasim for his constructive comments, discussions, and assistance in editing that contributed to this paper. We would also like to acknowledge the participants of the Clinton 1999 Project (H. McNairn et al.) for contributing Probe-1 data used in this paper.

6 REFERENCES

Chen, J.M., Pavlic, G., Brown, L., Cihlar, J., Leblanc, S., White, H.P., Hall, R., Peddle, D., King, D., Trofymow, J., Swift, E., Van der Sanden, J., and Pellikka, P.K.E., 2002, Derivation and validation of Canada-wide coarse-resolution leaf area index maps using high-resolution satellite imagery and ground measurements. *Remote Sensing of Environment*, 80, 165-184.

Bicheron, P. and Leroy, M., 1999, A method of biophysical parameter retrieval at global scale by inversion of a vegetation reflectance model. *Remote Sensing of Environment*, 67, 251-266.

Badhwar, G.D., MacDonald, R.B., Metha, N.C., 1986, Satellite-derived leaf-area-index and vegetation maps as input to global carbon cycle models – a hierarchical approach. *International Journal of Remote Sensing*, 7, 265-281.

Abuelgasim, A.A., Gopal, S., and Strahler, A.H., 1998, Forward and inverse modelling of canopy directional reflectance using a neural network, *International Journal of Remote Sensing*, 19(3), 453-471.

Abuelgasim, A.A , Gopal, S., Irons, J.R., and Strahler, A.H., 1996, Classification of ASAS multiangule and multispectral measurements using artificial neural networks, *Remote Sensing of Environment*, 57, 79-87.

Peddle, D.R., Hall, F.G., and LeDrew, E.F., 1999, Spectral mixture analysis and geometric-optical reflectance modelling of boreal forest biophysical structure, *Remote Sensing Environment*, 67, 288-297.

Broge, N.H., and Leblanc, E., 2000, Comparing prediction power and stability of broadband and hyperspectral vegetation indices for estimation of green leaf area index and canopy chlorophyll density, *Remote Sensing Environment*, 76, 156-172.

Goel, N.S., 1988, Models of vegetative canopy reflectance and their use in estimation of biophysical parameters from reflectance data, *Remote Sensing Reviews*, 32, 1-212.

White, H.P., Miller, J.R., and Chen, J.M., 2002, Four-scale linear model for anisotropic reflectance (FLAIR) for plant canopies. I: Model description and partial validation, *IEEE Transactions on GeoScience and Remote Sensing*, 39(5), 1072-1083.

Zarco-Tejada, P.J. and Miller, J.R., 1999, Land cover mapping at BOREAS using red edge spectral parameters from CASI imagery, *Journal of Geophysical Research*, 104(D22), 27921-27933.

Earth Search Sciences Inc., 2002, Technology - About Probe-1, *http://www.earthsearch.com*

Champagne, C.M., Staenz, K., Bannari, A., White, H.P., Deguise, J-C., and McNairn, H., 2002, Estimation of plant water content of agricultural canopies using hyperspectral remote sensing, Proceedings of the 1st International Symposium Recent Advances in Quantitative Remote Sensing held in Valencia, Spain, on 16-20 September 2002.

White, H.P., Miller, J.R., and Chen, J.M., 2002, Four-scale linear model for anisotropic reflectance (FLAIR) for plant canopies. II: Validation and inversion with CASI, POLDER, and PARABOLA data at BOREAS, *IEEE Transactions on GeoScience and Remote Sensing* – Invited paper, 40(5), 1038-1046.

Chen, J.M, and Leblanc, S.G., 1997, A four-scale bidirectional reflectance model based on canopy architecture, *IEEE Transactions on Geoscience and Remote Sensing*, 35, 1316-1337.

Hall, F.G., Townshend, J.R., and Engman, E.T., 1995, Status of remote sensing algorithms for estimation of land surface state parameters, *Remote Sensing of Environment*, 51, 138-156.

Beaudet, M., Messier, C., Canha,, C.D., 2002, Predictions of understorey light conditions in northern hardwood forests following parameterization, sensitivity analysis, and tests of the SORTIE light model, *Forest Ecology and Management*, 165, 235-248.

Sabol Jr., D.E., Gillespie, A.R., Adams, J.B., Smith, M.O., and Tucker, C.J., 2002, Structural stage in Pacific northwest forests estimated using simple mixing models of multispectral images, *Remote Sensing of Environment*, 80, 1-16.

Sellers, P.J., 1985, Canopy reflectance, photosynthesis and transpiration, *International Journal of Remote Sensing*, 6(8), 1335-1372.

Sellers, P.J., 1987, Reflectance, photosynthesis, and transpiration. II. The role of biophysics in the linearity of their interdependence, *Remote Sensing of Environment*, 21, 143-183.

Staenz, K., Szeredi, T. and Schwarz, J., 1998, ISDAS – A system for processing/analyzing hyperspectral data, *Canadian Journal of Remote Sensing*, 24(2): 99-113

Chen, J.M., Black, T.A., and Adams, R.S., 1991, Evaluation of hemispherical photography for determining plant area index and geometry of a forest stand, *Agricultural and Forest Meteorology*, 56, 129-143.

Vetterling, W.T., Teukolsky, S.A., Press, W.H., Flannery, B.P., 1990, Linear Programming and the Simplex Method, Numerical Recipes in C., Cambridge, U.K.: University Cambridge Press.

Dickinson, R.E., 1983, Land surface processes and climate-surface albedos and energy balance, *Advanced Geophysics*, 25, 205.

Sellers, P.J., Hall, F., Margolis, H., Kelly, B., Baldocchi, D., den Hartog, G., Cihlar, J., Ryan, M.G., Goodison, B., Crill, P., Ransonm K.J., Lettenmaier, D., and Wickland, D.E., 1995, The Boreal ecosystem-atmosphere study (BOREAS): An overview and early results from the 1994 field year, *Bulletin American Meteorological Society*, 76(9), 1549-1577.

Leblanc, S.G., Chen, J., White, H.P., Latifovic, R. Fernandes, R., Roujean, J-L., Lacaze, R., 2002, Mapping leaf area index heterogeneity over Canada using directional reflectance and anisotropy canopy reflectance models, Proceeding of the Joint 24th Canadian Symposium on Remote Sensing / 2002 International Geoscience and Remote Sensing Symposium held in Toronto, Ontario, Canada 24-28 June 2002.

White, H.P., Leblanc, S.G., Chen, J.M., Lacaze, R. and Roujean, J-L., 2001. Mapping biophysical parameters with modelled and inverted functions from directional satellite measurements, 23rd Canadian Symposium on Remote Sensing held in Ste. Foy, Quebec, Canada, 20-24 August, 2001.

Pacheco, A., Bannari, A., Deguise, J-C., McNairn, H., and Staenz, K., 2001, Application of hyperspectral remote sensing for LAI estimation in precision farming, Proceedings of the 23rd Canadian Symposium on Remote Sensing held in Ste. Foy, Quebec, Canada, 20-24 August, 2001, pp. 281-287.

LI-COR Inc., 1992, LAI-2000 Plant Canopy Analyser Operating Manual, LI-COR Inc., Lincoln Nebraska, USA.

GER Corporation, 2002, The GER3700 Field Portable Spectrometer, *http://www.ger.com/3700.html*

Peñuelas, J., Filella, I., Serrano, L., and Savé R., 1986, The reflectance at the 950-970 region as an indicator of plant water status, *International Journal of Remote Sensing*, 17(2), 373-382.